

Synthesis of single-phase Bi_4Te_3 -nanoparticles and nanostructures in the $\text{M}^{\text{IV}}\text{Te}$ - Sb_2Te_3 systems ($\text{M}^{\text{IV}} = \text{Sn}, \text{Pb}$)

D. Petri, M. Jastak, S. Schlecht

Institut für Chemie und Biochemie, Freie Universität Berlin, Germany

Contact author: petrid@zedat.fu-berlin.de

Abstract

We report the synthesis of single-phase nanoparticles of thermoelectric telluride materials in the binary Bi-Te system and the pseudo-binary $\text{M}^{\text{IV}}\text{Te}$ - Sb_2Te_3 systems ($\text{M}^{\text{IV}} = \text{Sn}, \text{Pb}$). The polydisperse binary samples were synthesised at low temperatures without surfactants, while the pseudobinary compounds resulted from annealing at 400 °C. All compounds showed good crystallinity. The ternary samples revealed the $\text{M}^{\text{IV}}\text{Te}$'s cubic NaCl-type structure while the lattice-constant was significantly smaller than the one of the original PbTe or SnTe respectively.

Introduction

Bi_4Te_3 was first described in 1831 as a mineral later named Pilsenite [1]. Since only mineralogists cared for the compound during the first seven decades of the 20th century it was synthesized for the first time by K. Yamana *et al.* in 1979 applying classical solid state chemistry melting methods [2]. Recent studies with bulk samples revealed a change from n- to p-type conduction at 175 K for this compound [3].

Most phases in the $\text{M}^{\text{IV}}\text{Te}$ - $\text{M}_2^{\text{V}}\text{Te}_3$ ($\text{M}^{\text{IV}} = \text{Ge}, \text{Sn}, \text{Pb}$; $\text{M}^{\text{V}} = \text{Sb}, \text{Bi}$) pseudobinary systems crystallize in the trigonal crystal systems. Only few compounds are known, were the $\text{M}^{\text{IV}}\text{Te}$'s cubic structures are retained, e.g. $\text{Pb}_{0.73}\text{Bi}_{0.18}\text{Te}$ [4]. Recent studies by Kanatzidis *et al.* on single-crystalline $\text{Pb}_{9.6}\text{Sb}_{0.3}\text{Te}_{10}$ lead to the assumption, that the M^{IV} -rich ternary compounds consist of a M^{IV} -rich matrix with M^{V} -rich nanoscale inclusions which altogether show an average NaCl-type

structure [5]. These results are consistent with investigations of the LAST-Materials which show similar nanoscale Sb-/Ag-rich inclusions in a PbTe-matrix which are held responsible for the exceptionally high ZT-values of this type of materials [6].

Experimental

PbTe, SnTe, Sb_2Te_3 and Bi_4Te_3 were synthesized according to [7]. The metal-chlorides were reduced with excess $\text{Li}(\text{Et}_3\text{BH})$ in THF at room temperature yielding metal-particles with a large surface.

The as produced activated elements M^* were reacted with Ph_2Te_2 as a soluble tellurium source using diglyme as a high boiling solvent. For PbTe, SnTe and Sb_2Te_3 reactions were carried out at 165 °C for 16 h. To produce Bi_4Te_3 , the reaction was carried out at 120 °C for 2 h. All products have been washed with THF several times and dried under vacuum.

To synthesise the pseudobinary M^{IV} -Sb-Te compounds stoichiometric mixtures of the binary phase nanoparticles were annealed under Ar at 400 °C for 17 h.

Powder-XRD pattern were recorded using a STOE StadiP powder diffractometer equipped with a Ge monochromator using $\text{Cu-K}\alpha$ radiation.

TEM micrographs were taken using a JEOL JEM-1010 100 kV electron microscope.

Results and Discussion

The synthesis of nc- Bi_4Te_3 yielded a very fine black powder, which is reasonably stable against air and moisture (Fig. 1).

The powder XRD pattern (Fig. 2) shows broad reflections which can be indexed according to the hexagonal structure of Bi_4Te_3 . TEM-micrographs show highly agglomerated nanocrystalline Bi_4Te_3 particles with particle sizes of about 20 – 50 nm, while the agglomerates show sizes in the range of several microns (Fig. 1).

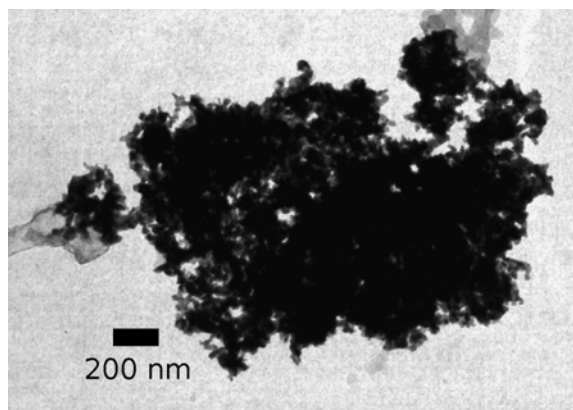


Fig. 1 TEM-micrograph of Bi_4Te_3 nanoparticles.

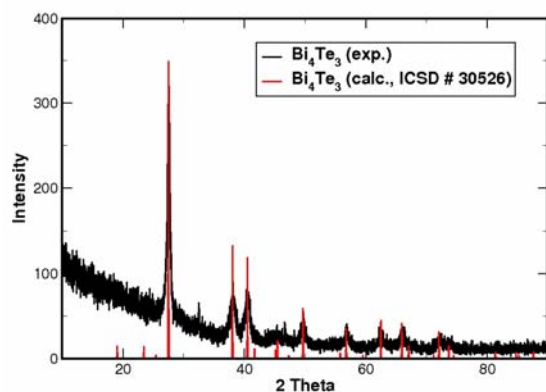


Fig. 2 Powder XRD pattern of nc- Bi_4Te_3 .

The experiments to produce ternary $\text{PbTe-Sb}_2\text{Te}_3$ and $\text{SnTe-Sb}_2\text{Te}_3$ compounds in the Pb-/Sn-rich areas of the phase diagrams yielded larger particles of about one micron in diameter (Figs. 3, 4). The powder XRD pattern could be indexed according to the NaCl-type structures of the group 14 metal tellurides. For both systems the ternary compounds revealed a change of the lattice constant. If compared with the lattice-constant of SnTe we find a reduction of the lattice-constant a of about 4.5 pm (Table 1) for $(\text{SnTe})_{10}(\text{Sb}_2\text{Te}_3)$.

Compound	a [Å]
SnTe	6.323(1)
$(\text{SnTe})_{10}(\text{Sb}_2\text{Te}_3)$	6.278(2)

Table 1 Lattice-constants of SnTe and $(\text{SnTe})_{10}(\text{Sb}_2\text{Te}_3)$.

Compound	a [Å]
PbTe	6.458(1)
$(\text{PbTe})_{20}(\text{Sb}_2\text{Te}_3)$	6.457(1)
$(\text{PbTe})_{10}(\text{Sb}_2\text{Te}_3)$	6.451(1)
$(\text{PbTe})_5(\text{Sb}_2\text{Te}_3)$	6.450(1)

Table 2 Lattice constants of pure PbTe and different ternary compounds.

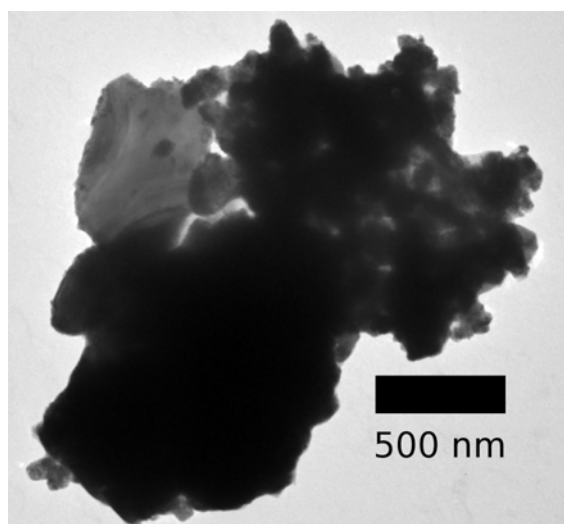


Fig. 3 TEM-micrograph of $(\text{SnTe})_{10}(\text{Sb}_2\text{Te}_3)$ particles.

For the ternary compounds in the $\text{PbTe-Sb}_2\text{Te}_3$ system there is a similar trend. The comparison of PbTe, $(\text{PbTe})_{20}(\text{Sb}_2\text{Te}_3)$, $(\text{PbTe})_{10}(\text{Sb}_2\text{Te}_3)$ and $(\text{PbTe})_5(\text{Sb}_2\text{Te}_3)$ also shows a slight change in a (Table 2, Figs. 5, 6). It may also be recognised that nc-PbTe is able to incorporate only about 10 mol-% of Sb_2Te_3 and that for higher concentrations of Sb_2Te_3 there is still a significant amount of unreacted Sb_2Te_3 to be seen in the powder pattern (Fig. 6).

The TEM-micrographs of the ternary compounds in both systems show a significant increase of the particle size. While the binary nanoparticles show diameters in the magnitude of 100 nm (Fig. 7) those of products are about ten times as large as a result of the interdiffusion process and general annealing phenomena.

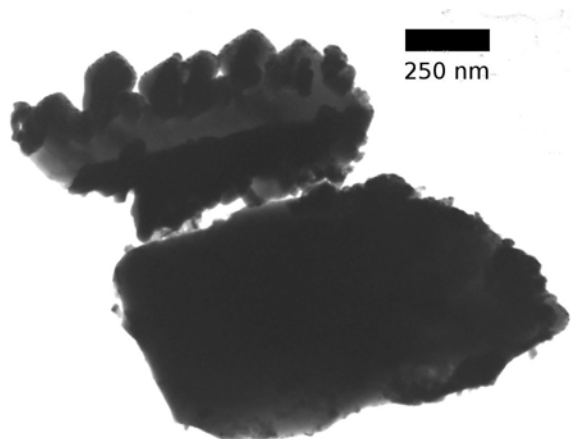


Fig. 4 TEM-micrograph of $(\text{PbTe})_{10}(\text{Sb}_2\text{Te}_3)$ particles.

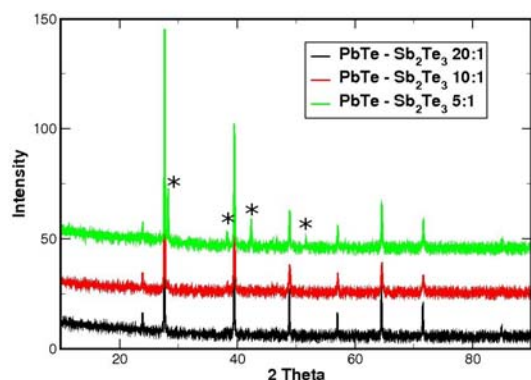


Fig. 5 XRD powder pattern of $(\text{PbTe})_{20}(\text{Sb}_2\text{Te}_3)$, $(\text{PbTe})_{10}(\text{Sb}_2\text{Te}_3)$ and $(\text{PbTe})_5(\text{Sb}_2\text{Te}_3)$ (* = unreacted Sb_2Te_3).

There are also density-fluctuations in the ternary agglomerates visible (Fig. 4). This suggests that there are probably also Sb-rich regions in a $\text{M}^{\text{IV}}\text{Te}$ -rich matrix. This makes this bottom-up approach promising for an improvement of thermoelectric properties due to enhanced phonon-scattering.

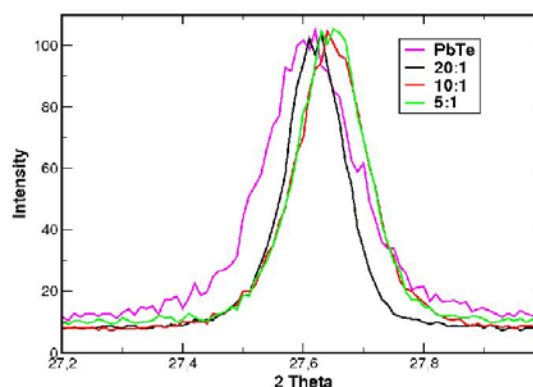


Fig. 6 Positions of the [200] reflections of PbTe, $(\text{PbTe})_{20}(\text{Sb}_2\text{Te}_3)$, $(\text{PbTe})_{10}(\text{Sb}_2\text{Te}_3)$ and $(\text{PbTe})_5(\text{Sb}_2\text{Te}_3)$ (normalised to 100%).

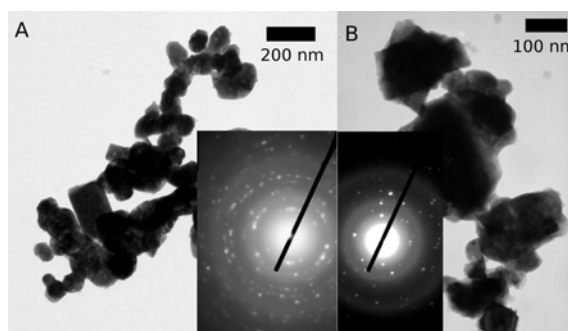


Fig. 7 TEM-micrographs of particles of the binary starting materials (A: PbTe; B: Sb_2Te_3).

References

- [1] T. Ozawa, H. Shimazaki, *Proc. Japan Acad. B* **58** (1982) 291.
- [2] K. Yamana, K. Kihara, T. Matsumoto, *Acta Cryst. B* **35** (1979) 147.
- [3] J. W. G. Bos *et al.*, *Phys. Rev. B* **75** (2007) 195203-1.
- [4] R. Chami *et al.*, *Revue de Chimie Minerale* **20** (1983) 305.
- [5] M. G. Kanatzidis *et al.*, *J. Am. Chem. Soc.*, **128** (2006) 14347.
- [6] M. G. Kanatzidis *et al.*, *J. Am. Chem. Soc.*, **127** (2005) 9177.
- [7] S. Schlecht, M. Budde, L. Kienle, *Inorg. Chem.* **41** (2002) 6001.